Supplementary material S3

In supplementary material 3, the results of the declustered samples without outliers for Regions A, B and C are presented. First, the samples were declustered from those with energy releases ≥ *M*5.5. The declustering method was as follows: if there were two energy releases ≥ *M*5.5 separated by ≤ 6 days, the larger energy release was retained. After the declustering process, the energy that belonged to outliers was removed to keep a fixed range of seismic energy before eliminating the space weather effects. There were two methods used to eliminate the space weather effects, which are described below:

1. Using the Dst index: This process was identical to that used in paper. If Dst was < −40 nT or the absolute value of the Dst difference from the previous 1-hour value was > 40 nT, the occurrence times of TEC anomalies from 1 day before to 4 days after this UT day (6 days in total) were not considered.

2. Considering Kp and F10.7: The condition that for days with at least one Kp > 3 (3o), the occurrence times of TEC anomalies were not considered was set. In addition, five periods of more strengthening solar activity, which were Dec. 18−24, 2014, Jan. 26−31, 2015, Mar. 7−8, 2015, Jun. 18−23, 2015, and Sep. 3−11, 2017, were found by using F10.7 and excluded (please see the following descriptions).

Since the F10.7 variation showed apparent periodicity with a solar rotation period of approximately 27 days, especially before 2017, this effect was retained in the analyses. The time series of the F10.7 difference between the observations and those one day before was computed, and the mean and standard deviation of the time series for the study period were found. Differences exceeding two standard deviations from the mean were identified, which had more rapid F10.7 variations and occurred in the five periods of more strengthening solar activity mentioned above. The Kp index was acquired from the International Service of Geomagnetic Indices (ISGI, http://isgi.unistra.fr/index.php), and F10.7 was acquired from Natural Resources Canada (https://spaceweather.gc.ca/solarflux/sx-5-en.php).

Figures S1—S12 show the results of correlation analyses of the TEC decrease anomaly and increase anomaly, using two methods to eliminate the space weather effects, for the declustered samples with energy releases ≥ *M*5.5 without outliers for Regions A, B and C, respectively. The parameters for using Dst and considering Kp and F10.7 are provided in Table S1 (similar to Table 2 in paper). The minimum *p* and the associated D, locations, and *r* for Figures S1—S12 are shown in Table S2.

In addition, we also examined the results of the declustered samples of seismic wave energy ≥ *M*5.5 released from the entire area of Regions A—C (13 °S—32.1 °N). We declustered the samples by the method mentioned above and retained and excluded the outliers. The same two methods were applied to eliminate the space weather effects. Since the occurrence times of TEC anomalies might have larger variability when using k =1.5 in the definition of TEC anomalies, k = 3 (a probability of 0.043 for an increase or decrease anomaly under a normal distribution) was used for analysis of energy released within the entire area of Regions A—C. The results are shown in Figures S13—S20. Table S3 shows the parameters of the declustered samples of energy ≥ *M*5.5 released within the entire Region A—C. Table S4 shows the minimum *p* and the associated D, locations, and *r* for Figures S13—S20.

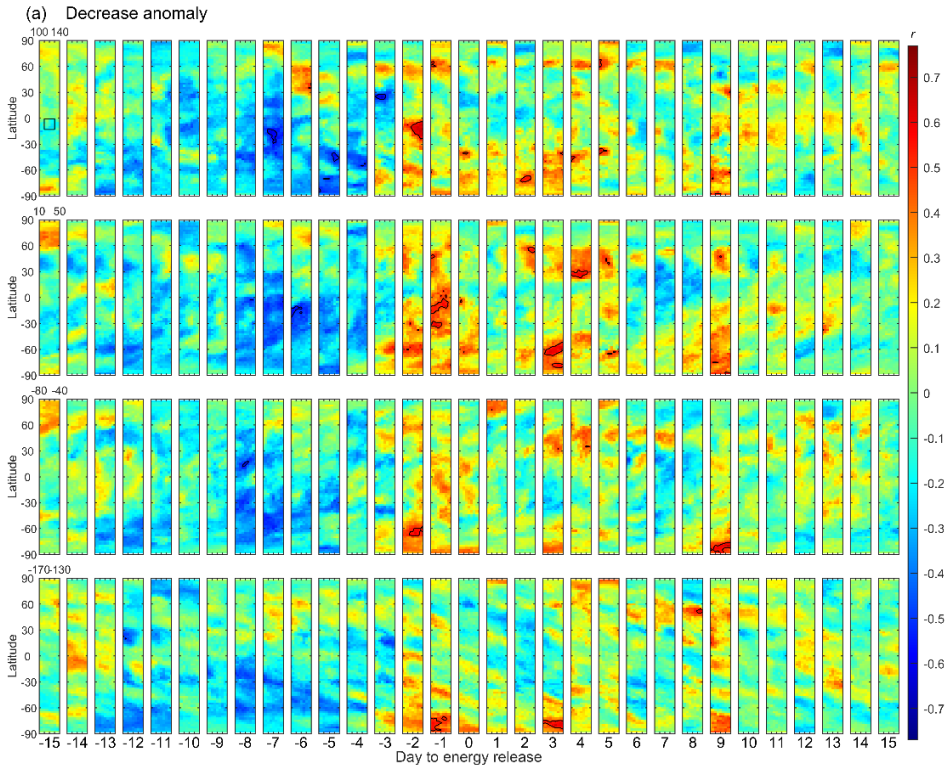

Figure S1. Distributions of the correlation coefficient of the TEC decrease anomaly for the declustered samples with energy releases ≥ *M*5.5 within Region A and without outliers. Data are removed using the Dst index.

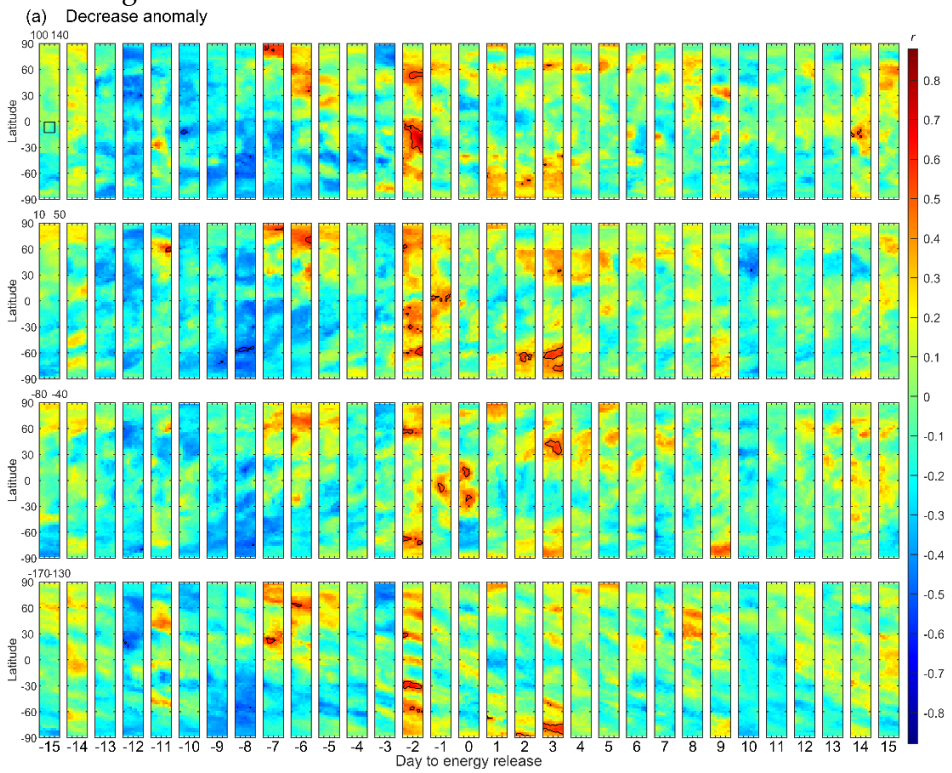

Figure S2. Same as Figure S1, but data are removed using Kp and F10.7.

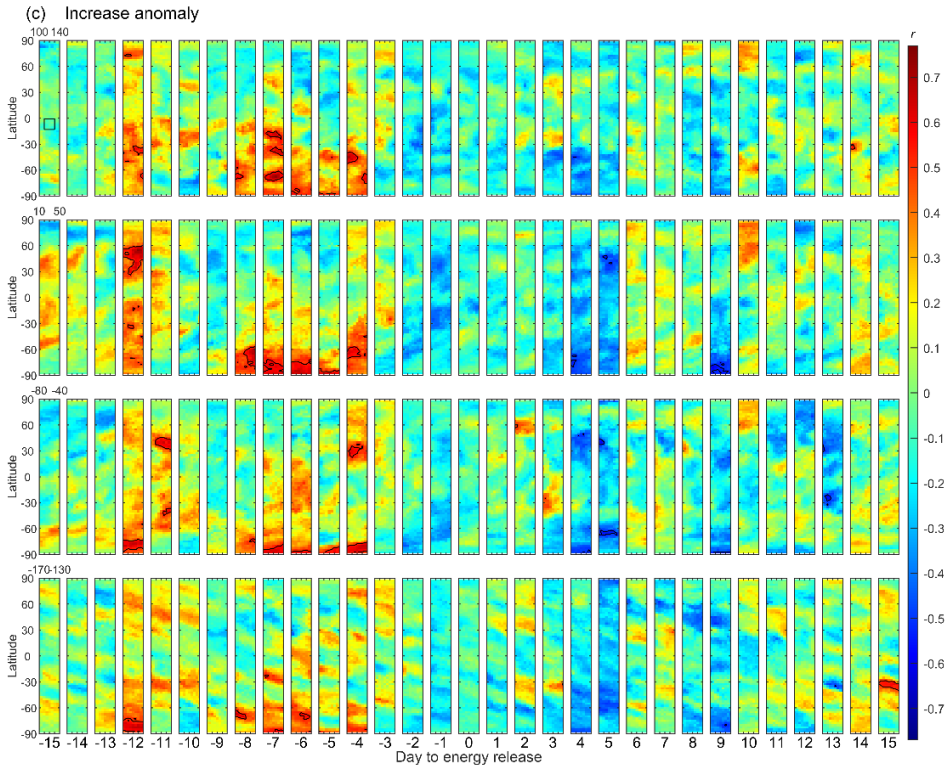

Figure S3. Distributions of the correlation coefficient of the TEC increase anomaly for the declustered samples with energy releases ≥ *M*5.5 within Region A and without outliers. Data are removed using the Dst index.

Figure S4. Same as Figure S3, but data are removed using Kp and F10.7.

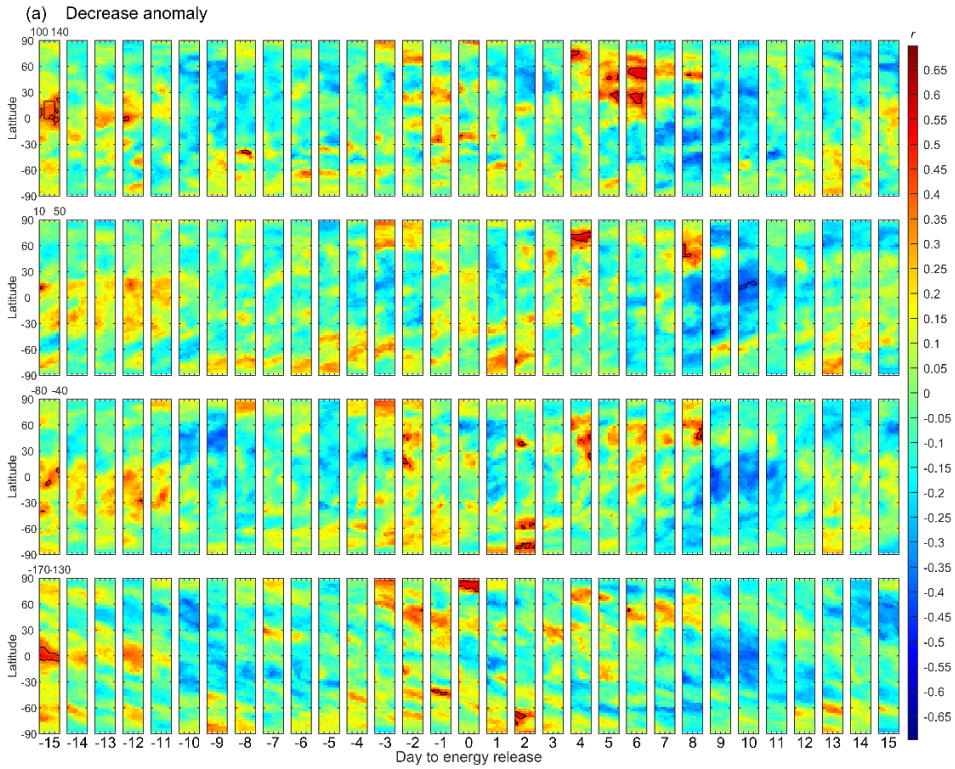

Figure S5. Distributions of the correlation coefficient of the TEC decrease anomaly for the declustered samples with energy releases ≥ *M*5.5 within Region B and without outliers. Data are removed using the Dst index.

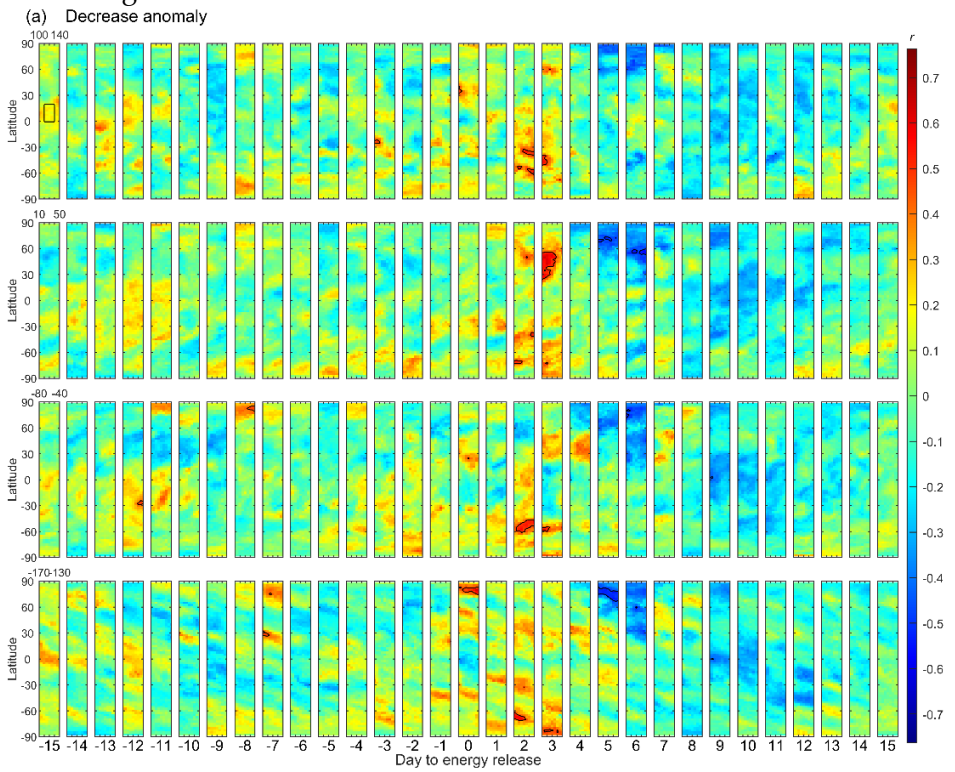

Figure S6. Same as Figure S5, but data are removed using Kp and F10.7.

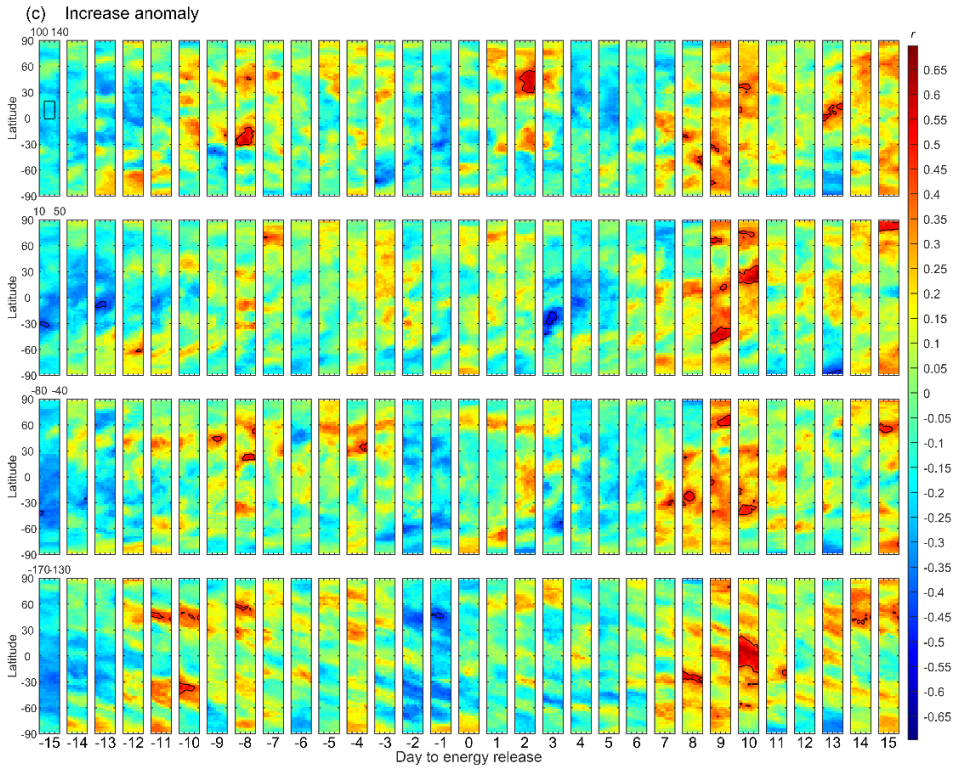

Figure S7. Distributions of the correlation coefficient of the TEC increase anomaly for the declustered samples with energy releases ≥ *M*5.5 within Region B and without outliers. Data are removed using the Dst index.

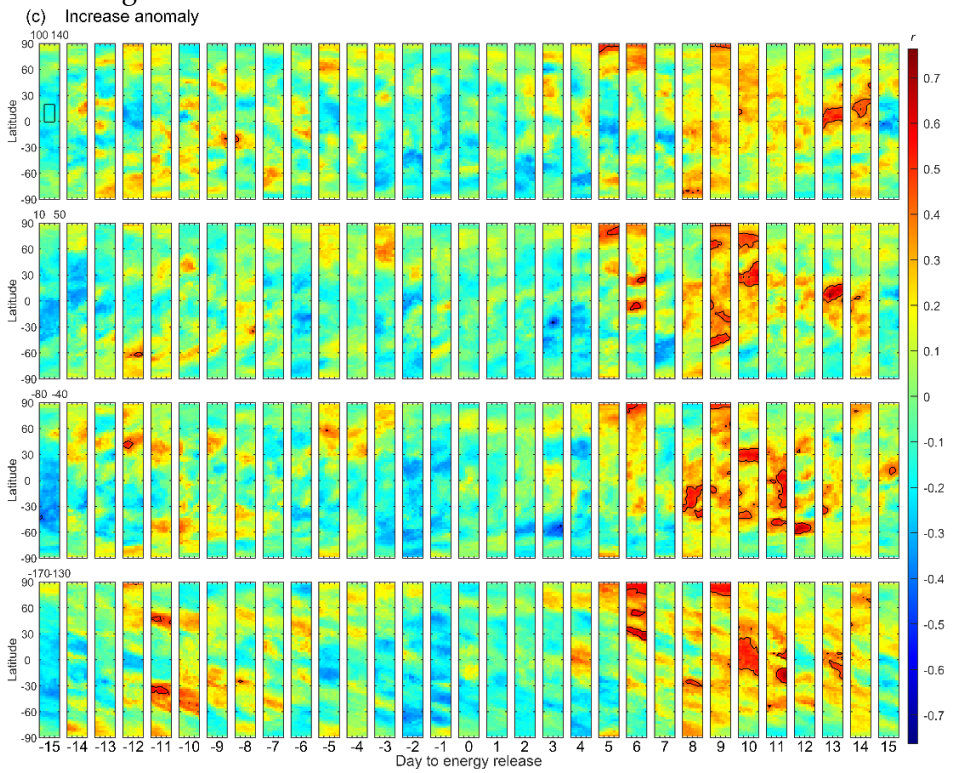

Figure S8. Same as Figure S7, but data are removed using Kp and F10.7.

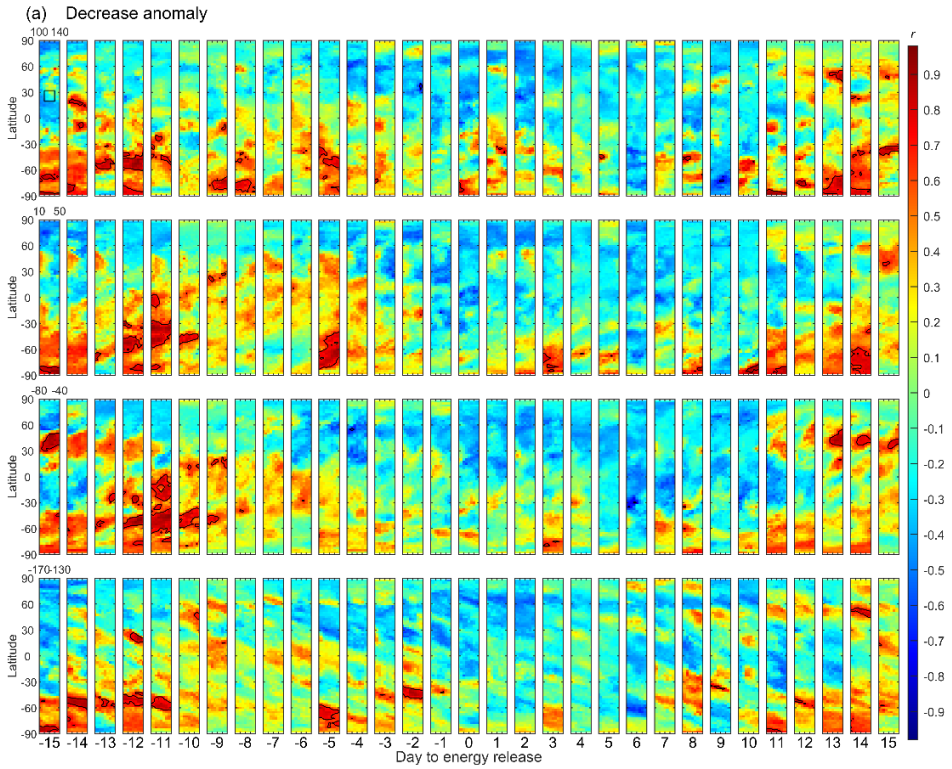

Figure S9. Distributions of the correlation coefficient of the TEC decrease anomaly for the declustered samples with energy releases ≥ *M*5.5 within Region C and without outliers. Data are removed using the Dst index.

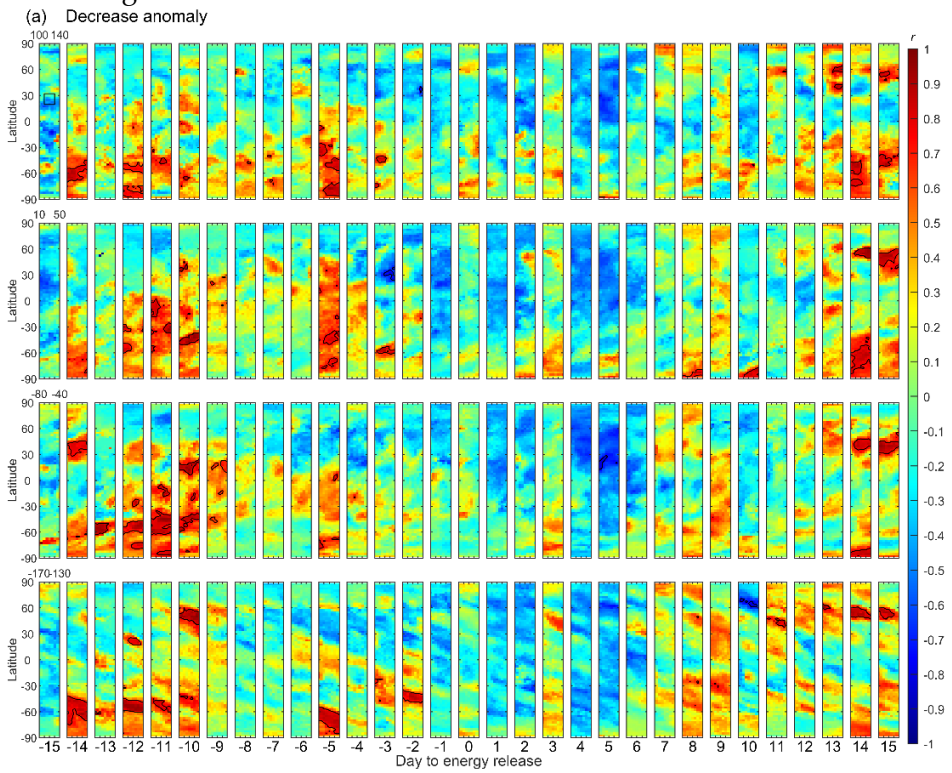

Figure S10. Same as Figure S9, but data are removed using Kp and F10.7.

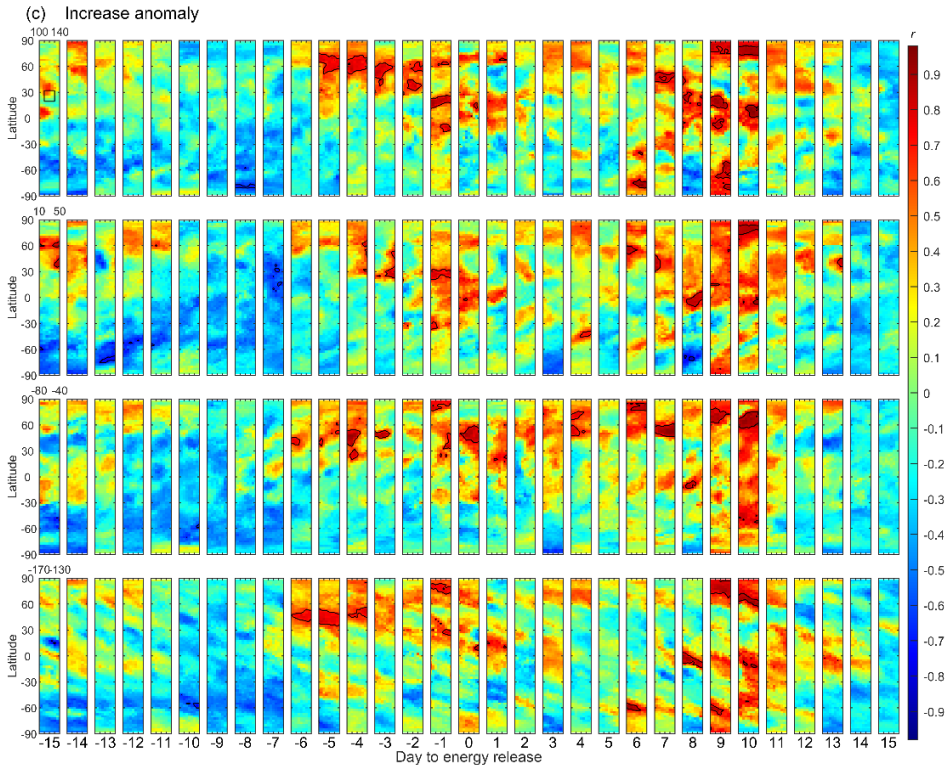

Figure S11. Distributions of the correlation coefficient of the TEC increase anomaly for the declustered samples with energy releases ≥ *M*5.5 within Region C and without outliers. Data are removed using the Dst index.

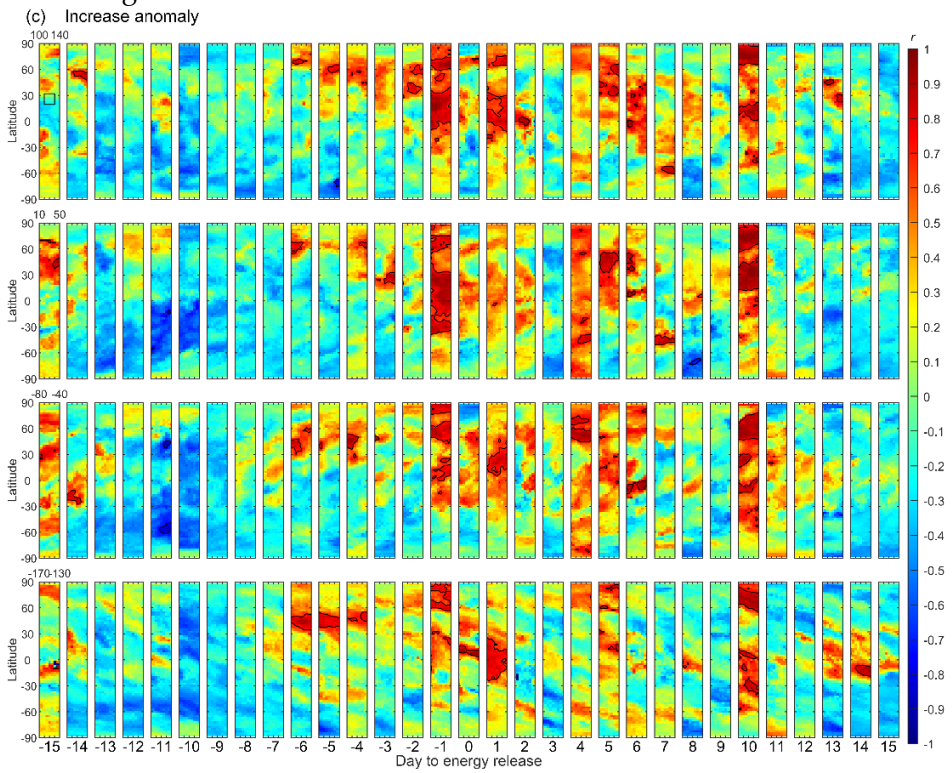

Figure S12. Same as Figure S11, but data are removed using Kp and F10.7.

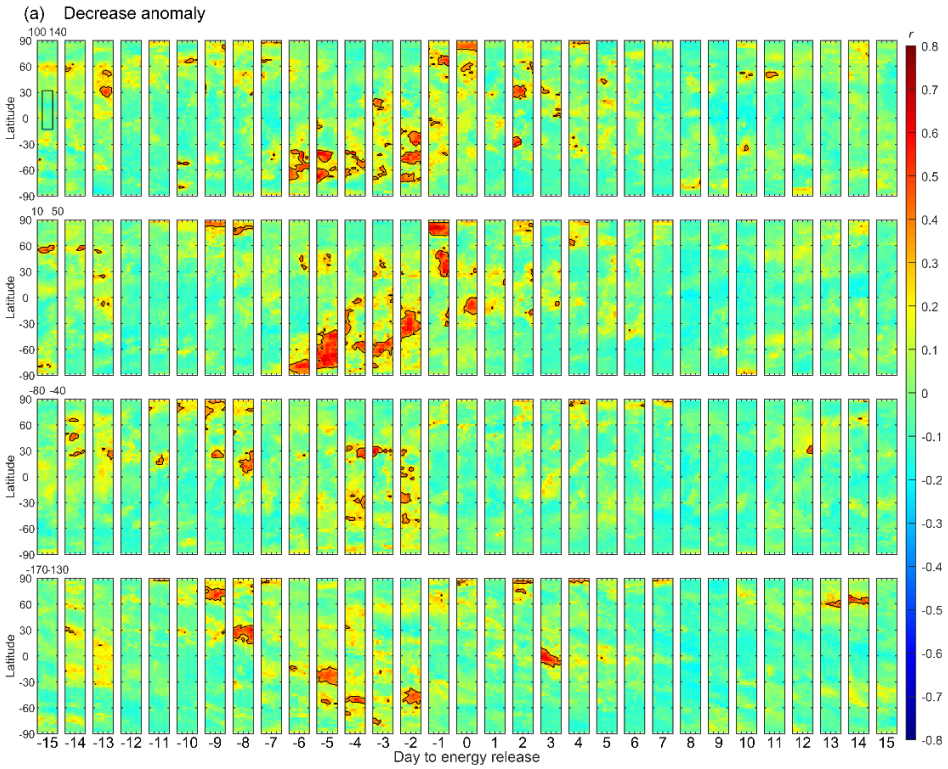

Figure S13. Distributions of the correlation coefficient of the TEC decrease anomaly (k = 3) for the declustered samples with energy releases ≥ M5.5 within the entire Region A—C and with outliers. Data are removed using the Dst index.

Figure S14. Same as Figure S13, but data are removed using Kp and F10.7.

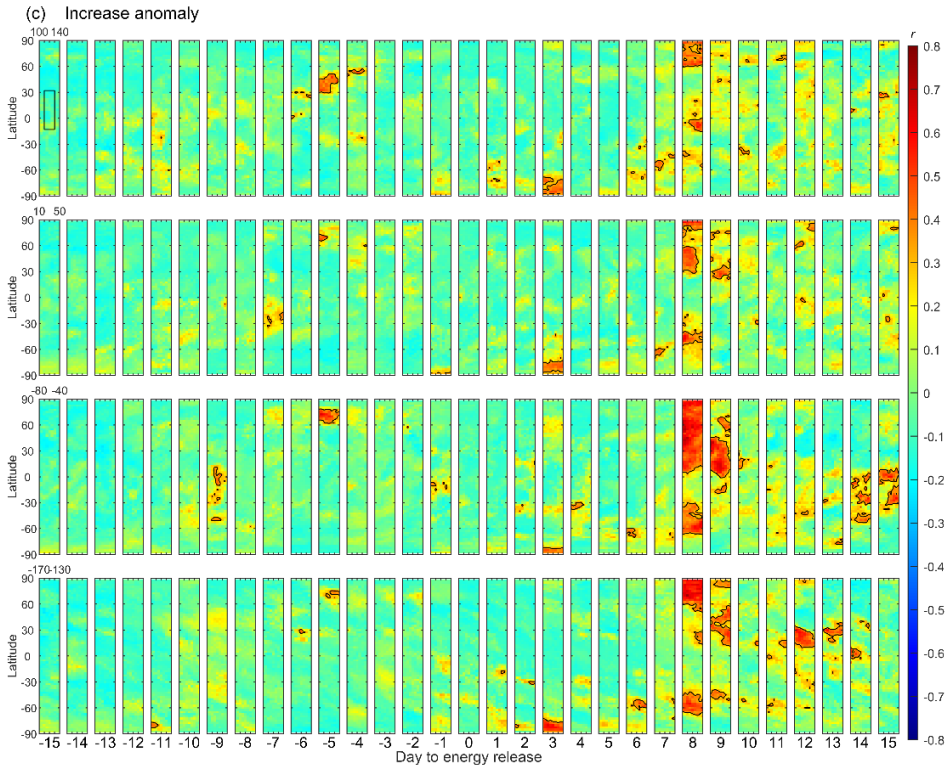

Figure S15. Distributions of the correlation coefficient of the TEC increase anomaly (k = 3) for the declustered samples with energy releases ≥ M5.5 within the entire Region A—C and with outliers. Data are removed using the Dst index.

Figure S16. Same as Figure S15, but data are removed using Kp and F10.7.

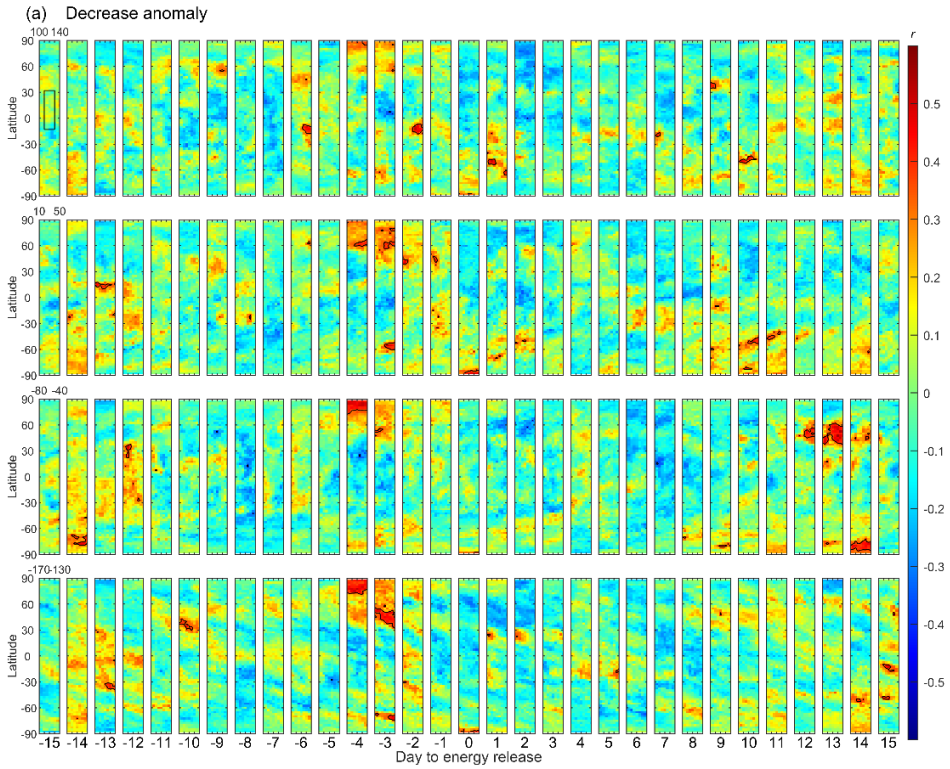

Figure S17. Distributions of the correlation coefficient of the TEC decrease anomaly (k = 3) for the declustered samples with energy releases ≥ M5.5 within the entire Region A—C and without outliers. Data are removed using the Dst index.

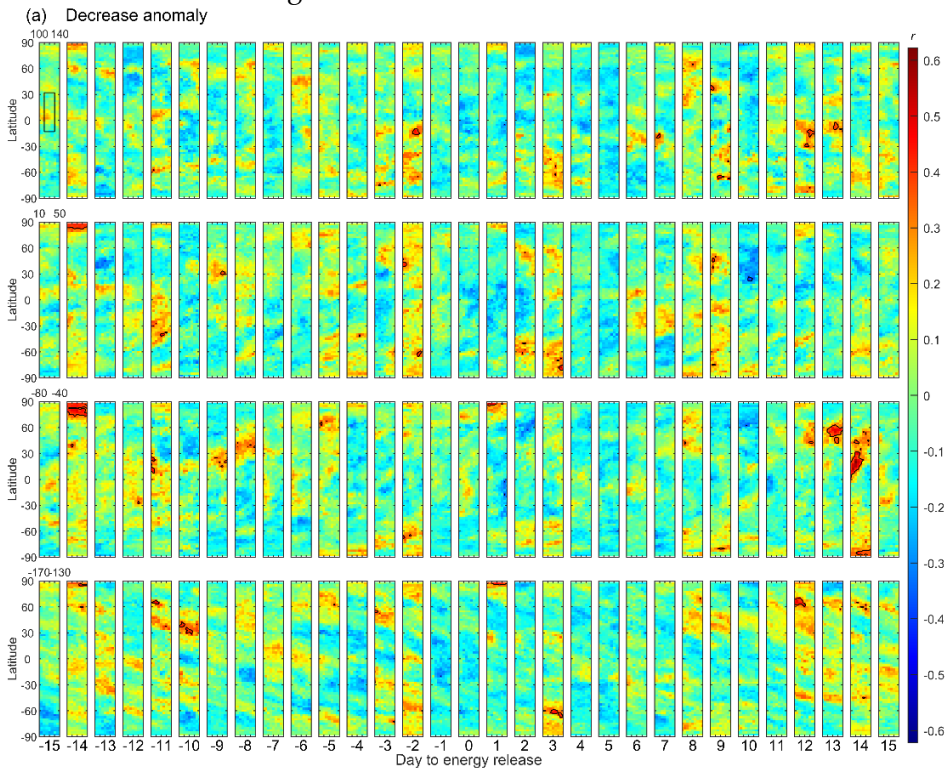

Figure S18. Same as Figure S17, but data are removed using Kp and F10.7.

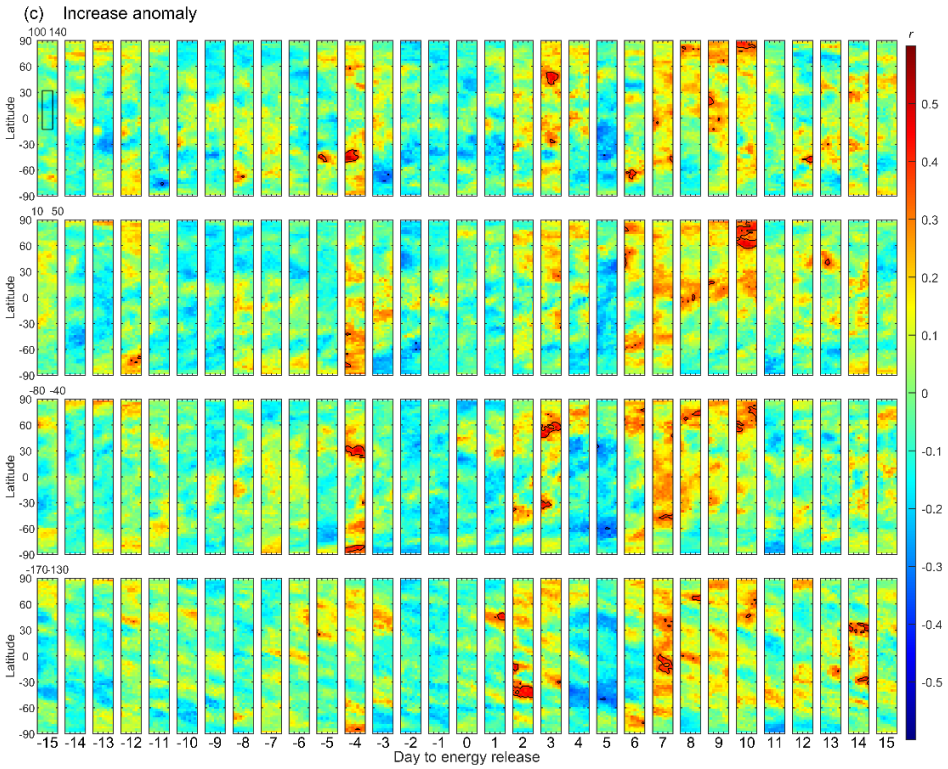

Figure S19. Distributions of the correlation coefficient of the TEC increase anomaly (k = 3) for the declustered samples with energy releases ≥ M5.5 within the entire Region A—C and without outliers. Data are removed using the Dst index.

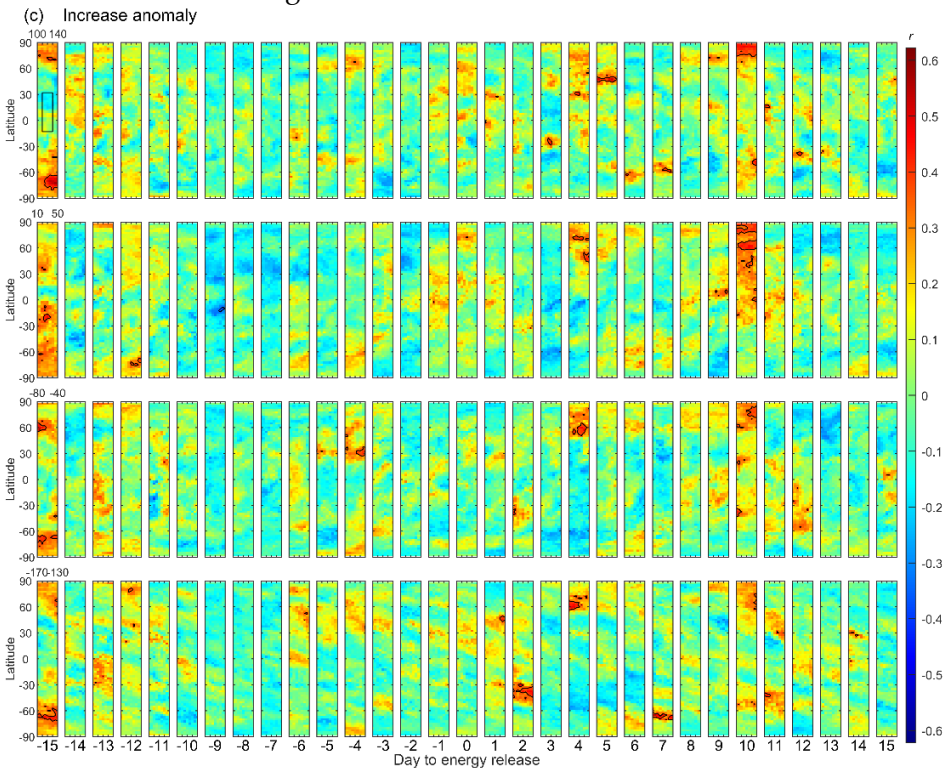

Figure S20. Same as Figure S19, but data are removed using Kp and F10.7.

Region	Using Dst			Using Kp and F10.7		
	Sample size	$r_{\alpha=0.01}$	**Max. daily energy release in *M***	**Sample size**	$r_{\alpha=0.01}$	**Max. daily energy release in *M***
A	20 - 28	0.479 - 0.561	6.480 - 6.512	18 - 28	0.479 - 0.590	6.425 - 6.512
B	25 - 37	0.418 - 0.505	6.201 - 6.307	24 - 39	0.408 - 0.515	6.104 - 6.307
C	8 - 14	0.661 - 0.834	6.429 - 6.429	8 - 16	0.623 - 0.834	6.117 - 6.429

Table S1. Parameters for the declustered samples of daily energy release equivalent to $M \geq 5.5$ earthquakes and without outliers. The left portion uses the Dst index, and the right portion uses Kp and F10.7 to eliminate the space weather effects.

			Min. *p*	D	Lat.	Long.	*r*
Region A	Using Dst index	Decrease anomaly	2.929E-05	4	-47.5	95	0.726
		Increase anomaly	7.909E-06	-12	55	40	0.750
	Using Kp and F107	Decrease anomaly	**3.391E-07**	**-2**	**-20**	**135**	**0.847***
		Increase anomaly	7.988E-07	-11	40	-45	0.879*
Region B	Using Dst index	Decrease anomaly	2.716E-05	8	52.5	-15	0.677
		Increase anomaly	1.607E-06	10	27.5	55	0.698*
	Using Kp and F107	Decrease anomaly	1.589E-05	2	-47.5	-20	0.692
		Increase anomaly	3.129E-08	13	5	25	0.763*
Region C	Using Dst index	Decrease anomaly	1.088E-07	-11	-35	10	0.959
		Increase anomaly	1.525E-06	-4	47.5	-75	0.934
	Using Kp and F107	Decrease anomaly	4.741E-08	-12	-50	-170	0.965
		Increase anomaly	**1.236E-07**	**-1**	**17.5**	**105**	**0.968**

Table S2. The minimum *p*, associated D, locations, and *r* for the results of declustered samples without outliers shown in Figures S1—S12. The bold font denotes the minimum *p* that appears before energy release and in the 120 °E sector. An asterisk near *r* denotes that the associated *r* is the maximum *r* during D = -15 to 15 and over the 5,183 GIM grids.

Region	Using Dst			Using Kp, and F10.7		
	Sample size	$r_{\alpha=0.01}$	**Max. daily energy release in *M***	**Sample size**	$r_{\alpha=0.01}$	**Max. daily energy release in *M***
A−C with outliers	56−64	0.320−0.342	7.300−7.507	48−64	0.320−0.368	7.002−7.507
A−C without outliers	48−56	0.342−0.368	6.507−6.542	41−58	0.336−0.398	6.508−6.542

Table S3. Same as Table S1, but for declustered samples of energy release ≥ *M*5.5 within the entire Region A−C and with and without outliers.

			Max. *p*	D	Lat.	Long.	*r*
A−C with outliers	Using Dst index	Decrease anomaly	1.504E-14	-5	-67.5	95	0.792*
		Increase anomaly	5.447E-13	8	62.5	-80	0.765*
	Using Kp and F107	Decrease anomaly	2.491E-14	-4	60	45	0.804*
		Increase anomaly	3.285E-18	13	-22.5	-115	0.841
A−C without outliers	Using Dst index	Decrease anomaly	2.463E-06	0	-87.5	65	0.582*
		Increase anomaly	**1.375E-05**	**-4**	**-47.5**	**110**	**0.551***
	Using Kp and F107	Decrease anomaly	2.575E-07	14	20	-70	0.622*
		Increase anomaly	**1.839E-05**	**-15**	**-72.5**	**135**	**0.569***

Table S4. Same as Table S2, but for the results shown in Figures S13−S20.